3D Finite Element Simulation to Predict the Induced Thermal Field in Case of Laser Cladding Process and Half Cylinder Laser Clad

Hussam El Cheikh[*1], Bruno Courant[2]

Institut de Recherche en Génie Civil et Mécanique (GeM) UMR CNRS 6183, LUNAM Université de Nantes, Ecole Centrale de Nantes, France

[*1]Hussam.elcheikh@univ-nantes.fr; [2]Bruno.courant@univ-nantes.fr

***Abstract*-- Direct Laser Fabrication (DLF) is a rapid manufacturing process based on laser cladding technique in which parts are fabricated layer by layer. In this work, a coaxial nozzle is used to deposit 316L stainless steel on a low carbon steel substrate. In order to obtain a 3D simulation with reasonable computation time, the thermal and geometrical problems are decoupled. The clad geometry is supposed to be a half cylinder which corresponds to a suitable geometry to build a part layer by layer. The finite element method is used to simulate the heat conduction in the part during the process with a 3D modelling using the Arbitrary Langrangian-Eulerian (ALE) in (Multiphysics Comsol 3.5). This model allows predicting the temperature field in the part during the process.**

Keywords*-- *Laser; Laser Cladding; Direct Laser Fabrication; Moving Heat Source; Finite Element Analysis; Thermal Field

I. INTRODUCTION

Direct Laser Fabrication (DLF) is a manufacturing method issue from rapid prototyping and laser technologies. Many works have been proposed to simulate the thermal field induced in a material heated by a moving laser beam during the 80's and 90's years. In the 2000's years many authors used these models more or less adapted to simulate the DLF process.

Rosenthal [1] proposed a 3D analytical function to describe the shape of the melt pool in the case of a moving heat source above a semi-infinite solid. El Cheikh et al. [2] have shown that the clad geometry is not controlled by the powder distribution into the jet. They propose [3] a phenomenological circular form model taking into account the surface tension forces between the protecting gases, the laser clad material and the substrate material. Oliveira and al. [4] present a theoretical and experimental study of the coaxial laser cladding process to understand relations between the process parameters and geometrical characteristics of one laser track. Picasso and Hoadley [5] proposed a two dimensional finite element model to calculate the melt pool shape for a known clad height. He and Mazumder [6] assumed a Gaussian distribution during the interaction between the powder feed rate and the laser beam, and Kar and Mazumder [7] proposed a one dimensional study for the dissolution of powder and mixing of the clad. Toyserkani and al. [8],[9] use a transient three-dimensional finite element modelling to show the influence of many parameters on the laser cladding process. Bamberger et al. [10] use a simplified theoretical model of Mie theory to show the influence of the injected particles on the heat flux and temperature distribution. Cline and Anthony [11] found the temperature distribution in the steady-state case using the Green's functions.

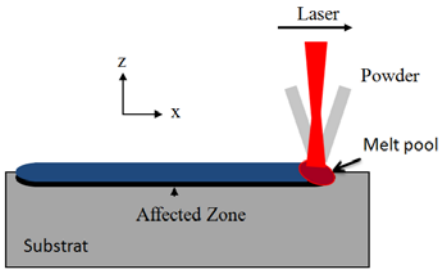

Figure 1 Model of direct laser fabrication

In this paper, a thermal simulation, using the Arbitrary Langrangian-Eulerian (ALE) mode, is used to access to the temperature distribution in the work piece and to simulate the clad layer geometry. The clad geometry is supposed to be a half cylinder which corresponds to a suitable geometry to build a part layer by layer. The thermal simulation is obtained by the calculation of the conduction equation

II. EXPERIMENTAL PROCEDURES

An easy way to comply with the journal paper formatting requirements is to use this document as a template and simply type your text into it.

A 5 axes speed machining is used associated with a fibre laser and a coaxial nozzle specially designed according to the laser beam characteristics. Argon, with a flow rate of 3l/min, carries the powder while a secondary gas, Argon with a flow rate of 5l/min, is shaping the powder stream. This nozzle is also equipped with a cooling channel to dissipate heat.

The laser beam is focused on the substrate surface while the powder stream focused plan is 5 mm above. The diameter of the focused powder jet is 0.6 mm and the focused laser diameter is 0.53mm at the substrate surface.

A 316L powder, with particles size between 45 and 75 µm, is used to realize single clad tracks. These experiments are realized with various parameters values. Three different powers (P =180, 280 and 360 W), three different powder

feed rates (Qm= 0.025, 0.05 and 0.075 g/s) and three different velocities (V= 300, 600 and 900 mm/min) are tested.

Figure 2 shows the conic powder jet stream geometry under the nozzle. Horizontal and vertical image analyses are studied. On the upper part of the jet, the horizontal image analysis displays two distributions due to the coaxial form of the nozzle. From the powder focus plan one distribution only remains. Image analysis software is used to study the powder distribution in the jet counting on the light reflection. The obtained functions are not directly the powder distribution in the jet but rather a projection of this distribution. Nevertheless, it can be deduced that, in the focus plan, the powder distribution is an almost symmetrical Gaussian type distribution. The vertical line displays the distribution along the z direction. As shown in the image analysis, the higher concentration of the powder stream is in the focus plan. The coaxial nozzle allows a perfect symmetry of the particles distribution in the stream and very few particles outside the main trajectories.

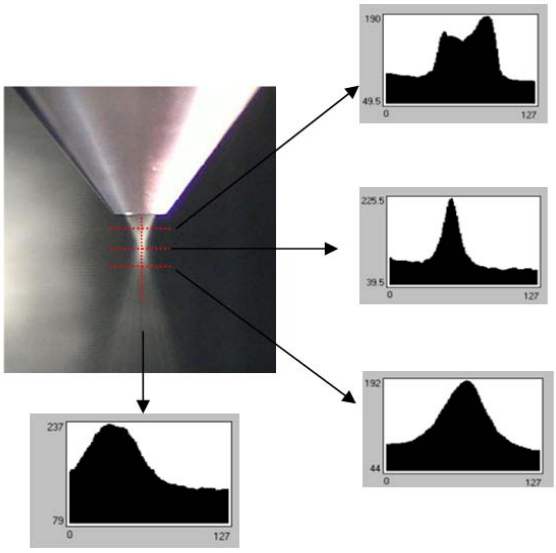

Figure 2 Powder distributions in the jet

The powder focus plan, at a distance l (l=3.5 mm) from the nozzle, is a disc with a diameter dp (dp=0.6 mm). The distance work L is fixed to 5 mm. Under the powder focus plan the powder distribution remains a Gaussian type distribution. The distance between the focus plan and the substrate surface is given by L-l (1.5 mm) and in the interaction plan the powder stream is 2 mm in diameter. The laser beam is focused on the substrate surface while the focused plan for the powder stream is 5 mm above.

III. Prediction of the Clad Geometry

El Cheikh et al. [2] studied the possibility to analytically relate the clad geometry and the powder distribution in the jet stream. They have established these relationships in case of three different distributions and have shown that the uniform distribution leads to semi cylindrical geometry. They have also shown that the powder accumulation induced by the powder distribution can't explain the clad geometry. The clad geometry is controlled by the tension forces which lead in all cases to a partial cylinder geometry. However the semi circular geometry is a particular case suitable to build a part layer by layer. In order to obtain an analytical description of the clad geometry, the analytical formulation established in [2] is used. The clad height h, in the end zone (interaction between the powder jet and the laser), is proportional to the powder feed rate, and in inverse proportion to the laser speed.

$$h = \frac{2P_e Q_m}{\rho \pi V r_p^{\,2}} \sqrt{r_p^{\,2} - y^2} - (x - Vt) \quad (1)$$

Where P_e is the powder efficiency, ρ is the material density and r_p is the radius of the interaction zone between the powder jet and the substrate.

H being the clad height after the laser nozzle past (Zone 2 in the figure 3), it is given by:

$$H = \frac{2P_e Q_m}{\rho \pi V r_p^{\,2}} \sqrt{r_p^{\,2} - y^2} \quad (2)$$

IV. Thermal Model

Arbitrary Langrangian-Eulerian (ALE) method allows the combination between the Eulerian formulation when the mesh is fixed and Langrangian formulation when the mesh moves with the matter to realize the clad laser.

Figure 3 shows the deformed mesh obtained with the ALE method under the nozzle and after it past. h is the clad laser height under the powder jet (Zone 1).

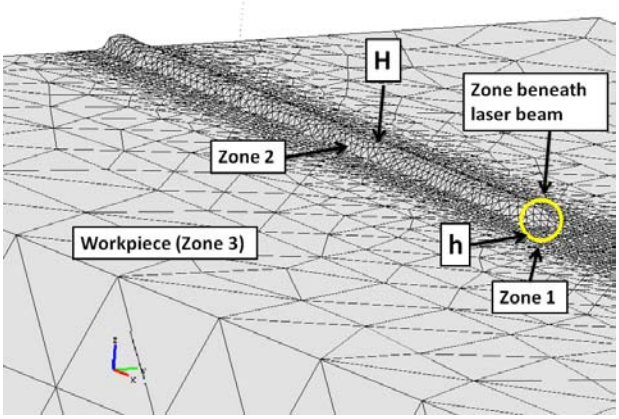

Figure 3 Deformed mesh with ALE method under and outside the laser beam

The induced thermal field during the DLF process is determined solving the heat conduction equation. The fundamental behaviour of heat conduction is that a flux Q (W/m3), representing the laser beam, heats the substrate surface.

The following assumptions are taken into account in the finite element model:

- The initial temperature of the substrate is 300K
- The heat source moves on the substrate surface at a velocity V
- Thermophysical proprieties for the 316L powder and the low carbon steel substrate depend on the

temperature.

- The latent heat of fusion and vaporization are assumed as 218 kJ/kg and 7600 kJ/kg respectively.

The transient temperature distribution T(x,y,z,t) is obtained from the following equation:

$$\rho.C_p.\frac{\partial T}{\partial t}+\nabla(-k.\nabla T)=Q \tag{3}$$

Where Cp is the specific heat capacity [J/kg.K], k is the thermal conductivity [W/m.K], t is the time [s].

The boundary condition on the surface area irradiated by laser beam (Zone 1) is given by:

$$-K.(\nabla T.n)=Q'-h_c(T-T_0)-\varepsilon.\sigma.(T^4-T_0{}^4) \tag{4}$$

And on the substrate but outside the laser beam (Zone 2,3) this condition is given by:

$$-K.(\nabla T.n)=-h_c(T-T_0)-\varepsilon.\sigma.(T^4-T_0{}^4) \tag{5}$$

Where Q' is the flux of energy [W/m2] Where hc is the heat convection coefficient [W/m2.K], where n is the normal vector of the surface, ε is the emissivity, σ is the Stefan-Boltzman constant [5.67 × 10-8 W/m2·K4] and T0 is the ambient temperature [K].

The initial condition for the transient analysis is

$$T(x,y,z,0)=T_0(x,y,z) \tag{6}$$

The heat source is assumed to be Gaussian on the clad front:

$$Q'=\frac{a\,P_0}{\pi\,r_f{}^2}\exp(-\frac{r^2}{r_f^2}) \tag{7}$$

Where $r=\sqrt{x^2+y^2}$, P_0 is the maximum power intensity, a is the absorptivity, $\frac{r_f^2}{2}$ is the variance of the Gaussian function.

The material change of state is taking into account with a Heaviside function:

$$x=x_s+(x_l-x_s)\ flc2hs(T-T_f,dT) \tag{8}$$

Where xs is the solid value, xl the liquid value, Tf the melting temperature, dT is the transition temperature between solid and liquid state, flc2hs is the Heaviside function.

TABLE I MATERIAL PROPRIETIES FOR SOLID AND LIQUID STATE

	Density [kg/m3]	Conductivity [W/(m.K)]	Specific heat [J/(kg.K)]
Solid state	7980	90	433
Liquid state	7551	12.29	734

The density and thermal conductivity for the solid state are those of the substrate while they are those of the 316L powder for the liquid state. For the specific heat Cp both the solid and liquid state values are those of the 316L stainless steel because it's mainly the powder that melt and solidify (Figure 4). The latent heat is taken into consideration through the specific heat expression by the following function:

$$C_p=C_{ps}+(C_{ps}-C_{pl})\ flc2hs(T-T_f,dT)+L_f\frac{\exp(-\frac{(T-T_f)^2}{(dT)^2})}{\sqrt{\pi\,(dT)^2}}+L_v\frac{\exp(-\frac{(T-T_v)^2}{(dT)^2})}{\sqrt{\pi\,(dT)^2}} \tag{9}$$

This effective expression is given in [12]. C_{ps} and C_{pl} are the specific heat of solid and liquid state respectively, L_f and L_v are the latent heat of fusion and vaporization respectively, T_v is the temperature of vaporization.

The first part of this expression ensures the latent heat variation between the solid and liquid states. In order to take into account that heat mainly diffuses in the substrate and considering that the main part of the liquid bath corresponds to the melted powder, C_p is the solid substrate one and C_{pl} the melted powder one. This way all nodes of the mesh follow the same expression and so there is no need to make time consuming and complex tests with the Arbitrary Langrangian-Eulerian (ALE) mode. The second part of this specific heat expression corresponds to the latent heat involves during the melting and vaporisation phenomena. With the same intention to do not slow down the computation speed and considering that the main part of the liquid bath corresponds to the melted powder L_f and L_v are the latent heat of fusion and vaporization of the powder. The exponential formulation is a smooth function numerically more suitable.

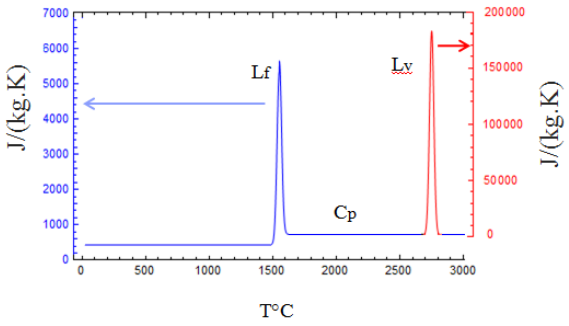

Figure 4 Specific heat with distinction between solid and liquid state and with latent heat of fusion Lf, and vaporization Lv

V. RESULT AND DISCUSSION

The thermal simulation of the laser cladding process shows a local melting pool. With the finite element simulation on Comsol, an absorptivity of 75% for the laser beam radiation is found to reproduce the form and dimensions of the melting pool. Among the 27 observed cross-sections, nine can be well simulated by a half-cylinder. All these experimental conditions have been simulated to validate our simulations.

Simulating the 3D melting pool during the clad process is a real challenge because it is a multi-physics complex

problem. The melted depth in the substrate is a very sensitive element which can be chosen to discuss the obtained results. Indeed, if one considers for example a laser speed decrease two opposite phenomenon occur. In one hand the linear deposit energy increase and so the melted depth in the substrate is expected to increase but in the other hand the linear deposit powder mass increase so the clad height increase and the thermal source moves away from the substrate so the melted depth in the substrate is expected to decrease. This competition can lead to apparent contradictory results.

Experimental and simulated depths of the melt pool are compared in table II.

For the lower powder feed rate (Table II, layer number a, b and c), experimental results show that the speed increase leads to a lower melted depth. The linear deposit energy phenomenon is predominant. In all other cases experimental and simulated results show that the laser speed increase leads to a melted depth increase. In these cases the second phenomena is predominant, the linear deposit powder mass decreases so the clad height decreases and the thermal source comes closer to the substrate and so the melted depth in the substrate increases.

Cases b, c, g, h and i appear as very acceptable. In the cases a, e and f differences between 70 and 100 micrometers are observed. Reported to the melted depth in the substrate, these differences are relatively important but if this modelling is used to predict the thermal field in the building part or in the substrate away from the melting pool the calculated thermal field can still correct. In case d the difference is real because no melting is predicted. The refined mesh dimensions could be insufficient to obtain the good result in this case.

TABLE II EXPERIMENTAL AND SIMULATED DEPTH OF THE MELTED POOL

Layer Number	Power (W)	Powder feedrate (g/s)	Velocity (m/s)	Experimental depth (mm)	Simulated depth (mm)
a	360	0.025	0.005	0.20	0.10
b	360	0.025	0.010	0.15	0.17
c	360	0.025	0.015	0.15	0.15
d	360	0.050	0.005	0.13	0
e	360	0.050	0.010	0.21	0.14
f	360	0.050	0.015	0.22	0.14
g	360	0.075	0.005	0.07	0.08
h	360	0.075	0.010	0.14	0.10
i	360	0.075	0.015	0.17	0.21

Figure 5 shows a simulation of the thermal field in the clad during the process in case b.

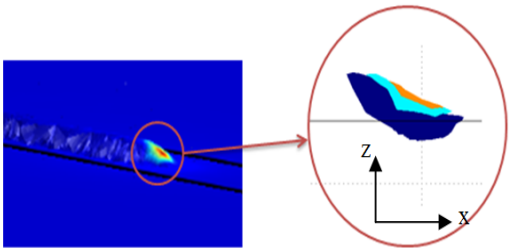

Figure 5 Melt pool view with the ALE method for the parameters (P=360 W, Qm=0.025 g/s and V=0.01 m/s)

The moving heat source is applied at the end of the depositing clad. Choosing the suitable geometry from the beginning, the considered complex problem is limited to a thermal one. The thermal field determination can be solved in the 3D space with fast calculus time taking into account the real geometry of the deposit clad. The delicate melted depth in the substrate is in most cases well simulated and the melting pool geometry can be simulated in 3D space.

Figure 6 shows in two cases a comparison between the experimental melt pool and the simulated one.

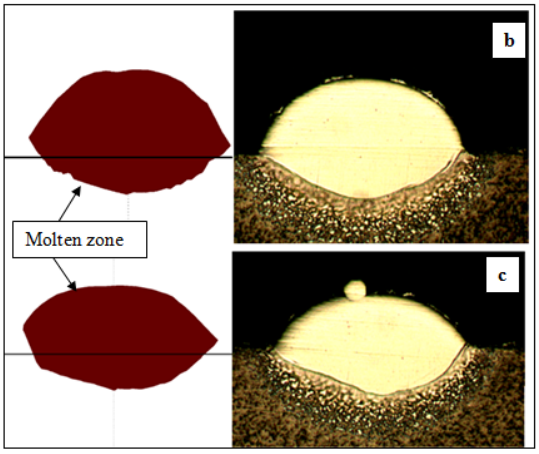

Figure 6 Cross sections of experimental results on the left and simulation results on the right showing the melt pool geometry in cases b and c.

Figure 7 shows the simulated thermal field in the plane (y,z)

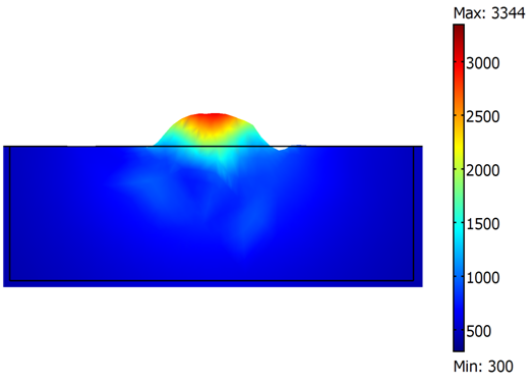

Figure 7 Thermal field in the plane (y,z) in the case f

VI. CONCLUSION

This paper presents a thermal simulation of the laser cladding process using the Arbitrary Langrangian-Eulerian (ALE) mode to represent the laser clad deposition. The conduction equation is solved to calculate temperature distribution. In most cases results show a good correlation between the calculated and observed melt pool geometries. The calculated thermal field could be used to optimize the process parameters in case of laser cladding process or direct metal laser fabrication. More directly, it helps to better understand the rule and intensity of the physical effects induced during the process as the laser speed effect on the melted depth. The next step is the prevision of the induced microstructures and constraints in the clad and the substrate.

REFERENCES

[1] D. Rosenthal, "Mathematical theory of moving sources of heat and its application to metal treatments," *Tans ASME* 68 pp. 849-866, 1946.

[2] H. El Cheikh, B. Courant, S. Branchu, J.Y. Hascöet, R. Guillén, "Analysis and prediction of single laser tracks geometrical characteristics in coaxial laser cladding process," *Opt Laser Eng*, 50, 3, pp. 413-422, 2012.

[3] H. El Cheikh, B. Courant, J.Y. Hascöet, R. Guillén, "Prediction and analytical description of the single laser track geometry in direct laser fabrication from process parameters and energy balance reasoning," *Journal of Materials Processing Technology* 212, pp. 1832-1839, 2012.

[4] U. de Oliveira, V. Ocelık, J.Th.M. De Hosson, "Analysis of coaxial laser cladding processing conditions," Surf. Coat. Technol. 197 pp.127–136, 2005.

[5] M. Picasso, A. F. A. Hoadley, "Finite element simulation of laser surface treatments including convection in the melt pool," *Int. J. Numerical methods for Heat and Fluid Flow* 4 pp. 61-83, 1994.

[6] X. He, J. Mazumder, "Transport phenomena during direct metal deposition," *Journal of Applied Physics* 101 pp. 053113, 2007.

[7] J. Mazumder, A. Kar, "Solid solubility in laser cladding," *Journal of Metals*, 39, pp. 18-23, 1987.

[8] E. Toyserkani, A. Khajepour, S. Corbin, "3-D finite element modeling of laser cladding by powder injection: effects of laser pulse shaping on the process," *Opt. Lasers Eng.* 41 pp. 849–867, 2004.

[9] E. Toyserkani, A. Khajepour, S. Corbin, "3-Dfinite element modeling of laser cladding by powder deposition: Effects of powder feed rate and travel speed on the process," *J. Laser Appl.* 15 3 pp.153–160, 2004.

[10] M. Bamberger, W.D. Kaplan, B. Medres, L. Shepeleva, "Calculation of process parameters for laser Alloying and cladding," *Journal of Laser Applications* 11 pp. 205-214, 1998.

[11] H.E Cline, T.R. Anthony, "Heat treating and melting material with a scanning laser or electron beam," *Journal of Applied Physics*, 48 pp.3895-3900, 1977.

[12] J.M.Jouvard, A.Soveja AND N.Pierron "Thermal modelling of metal surface texturing by pulsed laser", Proceedings of the European Comsol Conference 2006 in Paris, France, CD of proceedings].